Author(s): Tarkiainen, R. & Ahlskog, M. & Penttilä, J. & Roschier, L. & Hakonen, Pertti J. & Paalanen, M. & Sonin, E.

Title: Multiwalled carbon nanotube: Luttinger versus Fermi liquid

Year: 2001

Version: Final published version

Please cite the original version:

Tarkiainen, R. & Ahlskog, M. & Penttilä, J. & Roschier, L. & Hakonen, Pertti J. & Paalanen, M. & Sonin, E. 2001. Multiwalled carbon nanotube: Luttinger versus Fermi liquid. Physical Review B. Volume 64, Issue 19. 195412/1-4. ISSN 1098-0121 (printed). DOI: 10.1103/physrevb.64.195412

Multiwalled carbon nanotube: Luttinger versus Fermi liquid

R. Tarkiainen,[1] M. Ahlskog,[1] J. Penttilä,[1] L. Roschier,[1] P. Hakonen,[1] M. Paalanen,[1] and E. Sonin[1,2]
[1]*Low Temperature Laboratory, Helsinki University of Technology, FIN-02015 HUT, Finland*
[2]*The Racah Institute of Physics, The Hebrew University of Jerusalem, Jerusalem 91904, Israel*
(Received 23 July 2001; published 26 October 2001)

We have measured *IV* curves of multiwalled carbon nanotubes using end contacts. At low voltages, the tunneling conductance obeys non-Ohmic power law, which is predicted both by the Luttinger liquid and the environment-quantum-fluctuation theories. However, at higher voltages we observe a crossover to Ohm's law with a Coulomb-blockade offset, which agrees with the environment-quantum-fluctuation theory, but cannot be explained by the Luttinger-liquid theory. From the high-voltage tunneling conductance we determine the transmission line parameters of the nanotubes.

DOI: 10.1103/PhysRevB.64.195412 PACS number(s): 74.50.+r, 73.23.Hk, 73.40.Gk

Metallic carbon nanotubes are considered as outstanding realizations of strongly interacting, one-dimensional (1D) electron systems, i.e., Luttinger liquids (LL's).[1–3] A Luttinger liquid is a paramagnetic metal without Fermi-liquid quasiparticles. Its basic charged excitations are plasmons which can be viewed as propagating electrodynamic modes in a similar fashion as in any regular transmission line. Experimental evidence for LL behavior has recently been observed in single-walled carbon nanotubes[4] as well as in multiwalled tubes (MWNT's).[5] The transmission line analogy, in turn, facilitates the connection of LL theory to environment-quantum-fluctuation (EQF) theory.[6,7] This theory has been successful in explaining the Coulomb blockade in normal tunnel junctions.[7] Unlike the LL model, EQF theory incorporates various factors, which makes it much more amenable to detailed experimental comparison, especially in the case of resistive transmission lines.

In this paper we present experimental results on the *IV* curves for four metallic, arc-discharge-grown MWNT's. We analyze our results using both the EQF analysis[6,7] and the standard LL formulas.[8,9] At small voltages both of these approaches predict for *IV* curves a power law $I \propto V^{\alpha+1}$, which is also supported by experiments yielding $\alpha+1=1.23\pm0.1$. At large voltages we find that only EQF theory is applicable and obtain for the high-frequency impedance $Z=1.3$–$7.7\ \mathrm{k}\Omega$. From the values of α and Z we can independently determine the kinetic inductance of the nanotubes and obtain consistent values of $l_{kin}=0.1$–$4.2\ \mathrm{nH}/\mu\mathrm{m}$.

A multiwalled nanotube consists of several concentric nanotubes. About one-third of the tubes are expected to be metallic with quite large interlayer capacitance. According to our analysis, the large capacitance connects the inductive as well the resistive components of separate tubes in parallel. All metallic tubes take part in the conduction at high frequencies, in contrast to the Aharonov-Bohm experiments of Ref. 5 where only the outermost layer contributed to the dc resistance. The total electron density n of a MWNT is proportional to M, the number of metallic layers, and in each channel the Fermi velocity of 1D electron gas is $v_F=\pi\hbar n/4Mm^*=8\times10^5$ m/s. Here m^* is the effective mass of an electron, and we have taken into account the fact that each metallic layer has four independent 1D conduction channels.

A metallic nanotube, placed on a silicon substrate between metallic contact lines, can be viewed as an inner conductor of a transmission line whose outer conductor is formed by nearby metallic bodies. The capacitance per unit length of the line is $c=2\pi\epsilon\epsilon_0/\ln(r_g/r_0)$. Here ϵ is the dielectric constant of the medium between the conductors, r_0 is the outer radius of the nanotube, and r_g is a distance from a metallic ground. The current carriers of the nanotube occupy 1D conduction bands and, in contrast to the carriers in metallic wires, they have a low total density n, resulting in a large kinetic energy stored in the current flow. Therefore, the magnetic inductance $l_m=\mu_0\ln(r_g/r_0)/2\pi$, which is usually relevant for transmission lines, has to be replaced by the kinetic inductance $l_{kin}=m^*/ne^2$, since $l_{kin}\gg l_m$. In addition, for a 1D plasmon in a nanotube the inverse compressibility $d\mu/dn=m^*v_F^2/n$ of the neutral Fermi gas becomes comparable to the electrostatic inverse compressibility e^2/c of the transmission line geometry. This can be taken into account by renormalization of the nanotube capacitance into $\tilde{c}$:

$$\frac{1}{\tilde{c}}=\frac{1}{c}+\frac{1}{e^2}\frac{d\mu}{dn}=\frac{1}{c}+v_F^2 l_{kin}. \tag{1}$$

Hence, the plasmon velocity v_{pl} is

$$v_{pl}=\frac{1}{\sqrt{l_{kin}\tilde{c}}}=[1/l_{kin}c+v_F^2]^{1/2}, \tag{2}$$

and in the expression for the line impedance $Z=V/I$,

$$Z=\sqrt{l_{kin}/\tilde{c}}=l_{kin}v_{pl}=[l_{kin}/c+(R_K/8M)^2]^{1/2}, \tag{3}$$

V is the electrochemical (not only electric) potential difference, and $R_K=h/e^2$ is the quantum resistance.

In the above classical electrodynamic analysis the 1D plasmon modes are the only excitations of the nanotube transmission line. The LL model for an infinitely long MWNT (Refs. 8 and 9) recovers the electrodynamic plasmon mode with v_{pl} given by Eq. (2) [cf. the expression after Eq. (4) in Ref. 8]. But in addition to the plasmon mode, the Luttinger liquid has charge-neutral modes (a spin wave among them), which propagate with the velocity different from v_{pl} and keep the total charge density constant. The

TABLE I. Summary of our samples of single, metallic tubes T1–T4. $\mathcal{L}_1$ and $\mathcal{L}_2$ denotes the length of the tube over the metallic leads and the length of the free-standing section that is hanging $\sim$20 nm above the substrate, respectively. For sample T4, $\mathcal{L}_2$ specifies the length in contact with SiO_2. In the resistivity ratio $RR = R_0(4.2\ K)/R_0(290\ K)$, the values of R_0 have been obtained from slopes of the IV curves at $I=0$. T denotes the measurement temperature for the data in Figs. 1 and 2. The junction capacitance C_T and tunneling resistance R_T are taken from the IV-curve fits using Eq. (5). These fits also yield the lumped-element environmental impedance Z which is slightly different for positive and negative voltages. Kinetic inductance obtained from Z using $c=70$ aF/μm and Eq. (3) is given by l_{kin_Z}. The Luttinger-liquid power α is determined at $4<|V|<7$ mV. The kinetic inductance l_{kin_α} is an estimate obtained using Eq. (3). The voltage range of the tail fits is given in the last column.

	$\mathcal{L}_1/\mathcal{L}_2$ (μm)	RR	T (K)	R_T (kΩ)	C_T (aF)	Z (kΩ)	l_{kin_Z} (mH/m)	α	l_{kin_α} (mH/m)	Range (mV)
T1	0.8/0.5	1.7	4.2	25	31	3.5/7.7	0.9/4.2	0.30	1.1	10-50
T2	0.5/0.3	3.0	0.1	20	33	1.3/2.3	0.1/0.4	0.12	0.2	15-50
T3	0.8/0.6	4.6	4.2	46	37	2.0/4.8	0.3/1.6	0.32	1.2	10-50
T4	0.9/2.3	3.0	0.1	68	111	1.8/2.7	0.2/0.5	0.17	0.3	7-20

Coulomb interaction, measured by the difference of v_{pl}/v_F from unity, suppresses the single-electron density of state (DOS) $\rho(E)=dn/dE$ near the Fermi level. The DOS is given by the Fourier component of the electron Green's function $\langle\hat{\psi}(x,t)\hat{\psi}(x,0)^\dagger\rangle$ [$\hat{\psi}(x,t)$ is the electron operator] and is probed by the IV curve: $dI/dV\propto\rho(eV)$. At low energies $\rho(E)\propto E^{\alpha_L}$, where for an end-contacted infinitely long MWNT (Refs. 9 and 10)

$$\alpha_L=(v_{pl}/v_F-1)/4M. \tag{4}$$

In the limit of large M or no interaction $v_{pl}/v_F=1$, the IV characteristics of a MWNT approach Ohm's law ($\alpha_L=0$); i.e., the Luttinger liquid turns into a Fermi liquid.

Another approach, EQF theory, considers the effects of environment quantum fluctuations on IV characteristics under the conditions of a Coulomb blockade. A nonresistive, infinitely long nanotube acts as a dissipative environment, i.e., as a heat bath with which the tunneling electron can exchange energy.[6,7] The energy exchange is characterized by the function $P(E)$, which is a Fourier component of the correlator $\langle e^{i\hat{\varphi}(t)}e^{-i\hat{\varphi}(0)}\rangle$, where $\hat{\varphi}(t)$ is the operator of the phase. At $T=0$, $P(E)$ is proportional to the *second* derivative of the current: $d^2I/dV^2\propto P(eV)$. In the Coulomb blockade regime, i.e., when the voltage bias is less than e/C_T, where C_T is the capacitance of the tunnel contact, EQF theory predicts that $P(E)\propto E^{\alpha_E-1}$ and $I\propto V^{\alpha_E+1}$ with $\alpha_E=2\,\mathrm{Re}\{Z\}/R_K$. Using the impedance $Z=\sqrt{l_{kin}/\tilde{c}}$ of the nanotube, this yields the same power law as LL theory in the large-M limit. This fact, pointed out in Ref. 10, is not accidental. In the LL picture the current is suppressed because there are no single-electron quasiparticles, and the charge is transported by bosonic modes (plasmons). Although in a junction between 3D wires there are single-electron states available (in contrast to 1D), a tunneling electron at $V\ll e/C_T$ has not enough energy to get into them. As a result, the charge is transported again with 1D plasmons, which have similar properties for 1D and thin 3D wires.

On the other hand, one should expect a similarity between $\rho(E)$ and $P(E)$, since both operators $\hat{\psi}^\dagger$ and $e^{-i\hat{\varphi}}$, which define these two functions, are creation operators for the charge e. But if the exponents α_L and α_E for the conductance coincide, the exponents α_L and α_E-1 for $\rho(E)$ and $P(E)$, respectively, differ by 1. One can show,[11] however, that similar relations connect the $\rho(E)$ and $P(E)$ exponents with the impedance: $\alpha_L=2\mathrm{Re}\{Z_L\}/R_K-1$ and $\alpha_E-1=2\mathrm{Re}\{Z\}/R_K-1$. But due to charge-neutral modes, which were not considered in EQF theory, the nanotube impedance differs in LL theory from the impedance Z given by Eq. (3): $Z_L=Z+(4M-1)R_K/8M$. The difference in the impedance compensates for the difference in the relations connecting $\rho(E)$ and $P(E)$ with the conductance, and eventually in the large-M limit both theories predict the same exponent.

But the two approaches differ in their predictions for high voltages. According to EQF theory the power law is only valid in the Coulomb-blockade regime $\omega C_T\ll 1/Z$. The relevant frequency $\omega=eV/\hbar$ in this inequality corresponds to the environment mode excited by a tunneling event; in our experiments this means frequencies up to about 20 THz. At high frequencies and voltages the environmental impedance Z is shunted by the tunnel junction capacitance C_T and becomes $(i\omega C_T+1/Z)^{-1}$. Then EQF theory gives the formula[7]

$$I=\frac{1}{R_T}\left[V-\frac{e}{2C_T}+\frac{R_K}{Z}\left(\frac{e}{2\pi C_T}\right)^2\frac{1}{V}\right]. \tag{5}$$

This high-voltage asymptotics, characterized by the Coulomb offset $e/2C_T$ and the ''tail'' voltage $\propto 1/V$, was experimentally studied and discussed by Wahlgren *et al.* and Penttilä *et al.* within the horizon picture.[12,13] In contrast to EQF theory, in the LL approach the capacitance C_T of the tunneling contact is absent, and therefore this approach does not predict a crossover to the ''tail'' asymptotics given by Eq. (5).

A summary of our four nanotube samples, each with a diameter of about 15 nm, is presented in Table I. For contact, we employed gold electrodes which were evaporated either

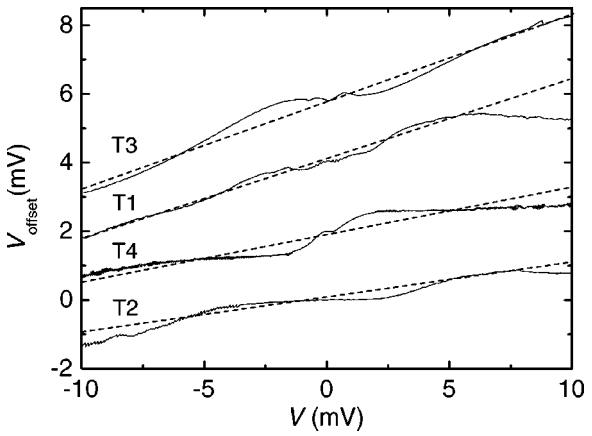

FIG. 1. Offset voltage $V_{offset}=V-I/(dI/dV)$ vs V for all our samples T1–T4; the power-law behavior $I\propto V^{\alpha+1}$ yields a straight line in this kind of a plot. The dashed lines illustrate linear fits made in the range $4<|V|<7$ mV. The effect of the Coulomb blockade near zero is seen to be small except for sample T4.

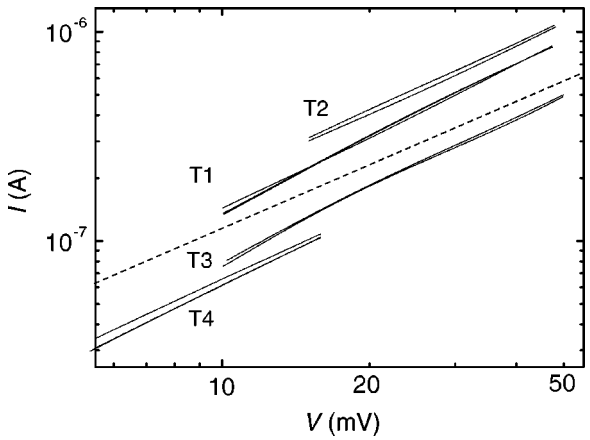

FIG. 2. High-voltage IV curves (both positive and negative polarities) on a log-log plot. The dashed line illustrates linear behavior ($\alpha=0$). For details, see text.

prior to or after the deposition of nanotubes. Deposition of nanotubes was done as described in Ref. 14. Mapping of nanotubes with respect to alignment marks as well as AFM micromanipulation was performed using Park Scientific Instruments Autoprobe CP. Chrome or titanium (2–3 nm layer) was employed as an attachment layer before evaporating gold. Vacuum brazing at 700 °C for 30 sec was employed to lower the contact resistance in samples T1–T3. On the dilution refrigerator, the samples were mounted inside a tight copper enclosure and the measurement leads were filtered using 0.5 m of Thermocoax cable.

Tunnel junction capacitances $C_T=31-111$ aF and resistances $R_T=20-68$ kΩ (neglecting the tube resistance) were determined from asymptotic behavior by fitting Eq. (4) to the measured IV curves. Owing to their relatively large size, the contacts to the nanotube are not ideal and may cause a small uncertainty in the interpretation of the α values. Namely, EQF theory and the LL model in the strong interaction and $M\gg 1$ limit predict 2 times smaller α values for the bulk than for the end contact.[7–9]

Figure 1 illustrates the low-voltage IV curve of all four samples T1–T4. We are plotting the quantity

$$V_{offset}=V-I\,\frac{dV}{dI}\ \text{vs}\ V,$$

which in the case of a power law yields a straight line with the slope $\alpha/(1+\alpha)$. Only a slight deviation of linear behavior is seen at low voltages in Fig. 1. This indicates that the Coulomb blockade of the island is rather weakly seen (except in T4). The linear behavior also implies that the two tunnel junctions become independent. At voltages $|V|>5$ mV, in spite of the additional wiggles, a slight tendency toward saturation is observed in the data. This is consistent with the EQF picture, which predicts that at high voltages V_{offset} must gradually approach to a C_T-dependent constant. By fitting a straight line through each data set at $4<|V|<7$ mV, we obtain $\alpha=0.23\pm0.1$ (Table I). Using Eqs. (2) and (3) we obtain $l_{kin_\alpha}=0.2-1.2$ nH/μm for the kinetic inductance. The capacitance for the nanotube, ~70 aF/μm is estimated using the average of $c=2C_T/\mathcal{L}$ where we employ the total tube length $\mathcal{L}$ for scaling.

Figure 2 displays IV curves measured at large voltages. In order to facilitate a direct comparison with the power-law dependence, we have plotted our results on a log-log scale. Our data are rather close to a single power law with small α but, at larger values of α (samples T1 and T3), there is a gradual approach toward a linear law as expected for a single junction in a resistive environment. Thus both figures give evidence that the environmental (EQF) theory is better suited for the analysis at high voltages. In fact, also the saturation observed by Bockrath *et al.*[4] can be explained by an asymptotic approach toward Ohm's law.

The plasma resonances, which one expects in finite nanotubes, are washed away in our samples. This gives a lower limit for the resistivity of the line, $r\mathcal{L}\geqslant Z/4$. On the other hand, the LC-line model works over our voltage range, i.e., $r\leqslant\omega l_{kin}$, which results in an upper limit for r of the order of 1 kΩ/μm (at 1 mV). For comparison, from the two-terminal resistance measurements we estimate that $r\lesssim 20$ kΩ/μm for our tubes at dc.[15]

One may argue that the poor agreement of the LL picture with the high-voltage part of the IV curves could be reconciliated by including the junction capacitance C_T in the impedance, as is done in EQF theory. There is, however, a conceptual problem to do it. The density of states, ρ, is expected to be a bulk property and, therefore, independent of C_T. Moreover, inclusion of C_T in the impedance, which determines ρ, does not help one to match the LL picture with experimental results. The capacitance C_T short-circuits the environment impedance, and $\rho(E)$ should decrease with E, like $P(E)$ in EQF theory. But since $dI/dV\propto\rho(E)$, in contrast with EQF theory where $dI^2/dV^2\propto P(E)$, this yields a high-voltage plateau (voltage-independent current), but not Ohm's law with Coulomb offset. The introduction of a proper high-energy cutoff in the LL model could explain a crossover to Ohm's law, but not a Coulomb offset. We expect this cutoff to be larger than the region of our analysis which is bounded by the presence of higher transverse modes above 50 mV.

Fits, based on Eq. (5), fall on top of the experimental data in Fig. 2. In the fitting, we assume that the junctions at the ends of the tube are symmetric and, in fact, I vs $V/2$ is fitted to the single-junction formula. We also tried to incorporate a cubic background ηV^3 in the fitting, which was found essential in Al samples because of the deformation of the tunnel barrier at high voltages.[13] Surprisingly, the cubic term was found negligible in all our nanotube samples. Our fits yield a characteristic impedance of $Z=1.3$–7.7 kΩ for the resistive environment. These results depend slightly on the measurement polarity (see Table I). Finally, using Eqs. (2) and (3), we obtain for the kinetic inductance $l_{kin}=0.1$–4.2 nH/μm.

Table I contains parameters obtained both from the EQF analysis for a LC-transmission line as well as from the power-law exponents according to the LL model. The results of the two methods overlap each other; the scatter of the power-law analysis is slightly smaller than that of the environmental analysis. In addition, we checked that the temperature dependence of the measured conductance, $dI/dV \propto T^{\alpha}$, yielded consistent values of $\alpha=0.25\pm0.1$. As a final result of all our determinations we quote the median value $l_{kin}=0.5$ nH/μm. If we compare this with the theoretical prediction $l_{kin}=R_K/8Mv_F$, we conclude that the average number of conducting layers in our nanotubes is 8 and the large variation of the inductance may come from the variation in M. The average value of 8 indicates that about every third layer in our nanotubes is metallic.

To conclude, on the basis of our experimental results we argue that, at high voltages, the environmental theory gives a better account of transport measurements of multiwalled nanotubes than the Luttinger-liquid picture, because the tunnel junction capacitance is neglected in Luttinger-liquid theory. At lower voltages, no distinction between these two theories can be made. Due to their large kinetic inductance, nanotubes provide an excellent high-impedance environment for normal junctions at high frequencies, which is crucial for single-electronics phenomena. As the kinetic inductances of different layers are in parallel in MWNT's, these phenomena will be more pronounced in single-walled carbon nanotubes.

Note added in proof. Recently we learned that M. Bockrath has considered the transmission line analogy in the context of carbon nanotubes. M. Bockrath, Ph.D. thesis (University of California, Berkeley, CA, 1999), unpublished.

We thank C. Journet and P. Bernier for supplying us with arc-discharge-grown nanotubes. Interesting discussions with B. Altshuler, F. Hekking, G.-L. Ingold, A. Odintsov, and A. Zaikin are gratefully acknowledged. This work was supported by the Academy of Finland, by the Israel Academy of Sciences and Humanities, and by the Large Scale Installation Program ULTI-3 of the European Union.

[1] See, e.g., ''Special Issue on Nanotubes'' in Phys. World **13**(6), 29 (2000).

[2] C. Dekker, Phys. Today **52** (5), 22 (1999).

[3] See, e.g., M. P. A. Fischer and L. I. Glazman, in *Mesoscopic Electron Transport*, edited by L. L. Sohn, L. P. Kouwenhoven, and G. Schön (Kluwer Academic, Dordrecht, 1997), p. 331; J. Voigt, cond-mat/0005114 (unpublished).

[4] M. Bockrath, D.H. Cobden, J. Lu, A.G. Rinzler, R.E. Smalley, L. Balents, and P.L. McEuen, Nature (London) **397**, 598 (1999).

[5] C. Schönenberger, A. Bachtold, C. Strunk, J.-P. Salvetat, and L. Forro, Appl. Phys. A: Mater. Sci. Process. **69**, 283 (1999); A. Bachtold, C. Strunk, J.-P. Salvetat, J.-M. Bonard, L. Forro, T. Nussbaumer, and C. Schönenberger, Nature (London) **397**, 673 (1999).

[6] M.H. Devoret, D. Esteve, H. Grabert, G.-L. Ingold, H. Pothier, and C. Urbina, Phys. Rev. Lett. **64**, 1824 (1990).

[7] G.-L. Ingold and Yu. V. Nazarov, in *Single Charge Tunneling*, edited by H. Grabert and M. H. Devoret (Plenum Press, New York, 1992), pp. 21–107.

[8] C. Kane, L. Balents, and M.P.A. Fisher, Phys. Rev. Lett. **79**, 5086 (1997).

[9] R. Egger, Phys. Rev. Lett. **83**, 5547 (1999).

[10] K.A. Matveev and L.I. Glazman, Phys. Rev. Lett. **70**, 990 (1993).

[11] E.B. Sonin, cond-mat/0103017 (unpublished).

[12] P. Wahlgren, P. Delsing, and D.B. Haviland, Phys. Rev. B **52**, R2293 (1995); P. Wahlgren, P. Delsing, T. Claeson, and D.B. Haviland, *ibid.* **57**, 2375 (1998).

[13] J.S. Penttilä, Ü. Parts, P.J. Hakonen, M.A. Paalanen, and E.B. Sonin, Phys. Rev. B **61**, 10 890 (2000).

[14] L. Roschier, J. Penttilä, M. Martin, P. Hakonen, M. Paalanen, U. Tapper, E. Kauppinen, C. Journet, and P. Bernier, Appl. Phys. Lett. **75**, 728 (1999).

[15] The ballisticity of our tubes is enhanced by the AFM manipulation which seems to clean the surface. This is in accordance with the work of S. Frank, P. Poncharal, Z.L. Wang, and W.A. de Heer, Science **280**, 1744 (1998), in which ballistic propagation in MWNT's was observed after dipping into a Hg bath.